

# The effect of element substitution on high-temperature thermoelectric properties of $\text{Ca}_3\text{Co}_2\text{O}_6$ compounds

Masashi Mikami<sup>a,b,\*</sup>, Ryoji Funahashi<sup>a,b</sup>

<sup>a</sup>National Institute of Advanced Industrial Science and Technology, The Research Institute of Ubiquitous Energy Devices, 1-8-31, Midorigaoka, Ikeda, Osaka 563-8577, Japan

<sup>b</sup>CREST, Japan Science and Technology Agency, 4-1-8, Honcho Kawaguchi, Saitama 332-0012, Japan

Received 29 December 2004; received in revised form 26 February 2005; accepted 6 March 2005

## Abstract

Polycrystalline  $\text{Ca}_3\text{Co}_{1.8}\text{M}_{0.2}\text{O}_6$  ( $M = \text{Mn}, \text{Fe}, \text{Co}, \text{Ni}, \text{Cu}$ ) and  $\text{Ca}_{2.7}\text{Na}_{0.3}\text{Co}_2\text{O}_6$  were synthesized by solid-state reaction to evaluate the effect of substitution on the thermoelectric properties of  $\text{Ca}_3\text{Co}_2\text{O}_6$ . Substitution by Mn, Cu and Na appears to increase carrier density, given that electrical resistivity ( $\rho$ ) and the Seebeck coefficient ( $S$ ) were simultaneously reduced. Conversely, Fe substitution seems to reduce carrier density, resulting in a simultaneous increase in  $S$  and  $\rho$ . Cu and Na substitution resulted in a significant decrease in  $\rho$  due to enhancement of grain size and grain boundary connectivity, which could have a strong impact on  $\rho$ . Not only the intrinsic substitution effect on the electronic state but also this modification of the microstructure plays an important role in improvement of the thermoelectric power factor, particularly in the case of the Na-substituted sample.

© 2005 Elsevier Inc. All rights reserved.

**Keywords:**  $\text{Ca}_3\text{Co}_2\text{O}_6$ ; Thermoelectric compound; Cobaltite; Oxide; Polycrystal; Solid-state reaction; Microstructure; Element substitution

## 1. Introduction

Thermoelectric devices have recently attracted renewed interest in terms of their potential application to clean energy-conversion systems. The conversion efficiency of a thermoelectric material is evaluated according to its figure of merit, defined as  $Z = S^2/\rho\kappa$ , where  $S$  is the Seebeck coefficient,  $\rho$  is the electrical resistivity and  $\kappa$  is the thermal conductivity. Oxides have thus been regarded as unsuitable for thermoelectric application because of their high electrical resistivity resulting from poor carrier mobility. However, the recent discovery of large thermopower coexisting with low  $\rho$  in layered cobaltites of  $\text{Na}_x\text{CoO}_2$  and  $\text{Ca}_3\text{Co}_4\text{O}_9$  (Co349) has

opened the way to exploration of oxide thermoelectric materials [1–5]. Single crystals of these cobalt oxides exhibit good thermoelectric performance, characterized by a dimensionless figure of merit ( $ZT$ , where  $T$  is absolute temperature) of  $> 1$  at 1000 K [2,4], competitive with conventional degenerate semiconductors such as  $\text{Bi}_2\text{Te}_3$ ,  $\text{PbTe}$  and  $\text{Si}_{1-x}\text{Ge}_x$ . In addition, we have reported that  $\text{Ca}_3\text{Co}_2\text{O}_6$  (Co326), which is a decomposed phase of Co349 and stable up to 1300 K [6], has potential as a thermoelectric material for use at temperatures higher than the decomposition temperature of Co349 [7]. However, the  $ZT$  of Co326, 0.15 at 1073 K, fails to meet the  $ZT > 1$  criterion for practical use as a thermoelectric material, making it necessary to improve the thermoelectric properties of this system. Some research groups have reported the effect of substitution on the physical properties of the Co326 system [8–11] and have indicated the possibility of using element substitution to improve its thermoelectric performance. In the present study, the effects of partial

\*Corresponding author. National Institute of Advanced Industrial Science and Technology, The Research Institute of Ubiquitous Energy Devices, 1-8-31, Midorigaoka, Ikeda, Osaka 563-8577, Japan.  
Fax: +81 72 751 9622.

E-mail address: [m-mikami@aist.go.jp](mailto:m-mikami@aist.go.jp) (M. Mikami).

element substitutions (Mn, Fe, Ni and Cu for the Co site and Na for the Ca site) on the thermoelectric properties of the Co326 system are examined over a temperature range of 300–1073 K using polycrystalline specimens.

## 2. Experimental procedure

Polycrystalline  $\text{Ca}_3\text{Co}_{1.8}\text{M}_{0.2}\text{O}_6$  ( $M = \text{Mn, Fe, Ni and Cu}$ ) and  $\text{Ca}_{2.7}\text{Na}_{0.3}\text{Co}_2\text{O}_6$  samples were synthesized by solid-state reaction. Powders of  $\text{CaCO}_3$ ,  $\text{Co}_3\text{O}_4$ ,  $\text{Mn}_2\text{O}_3$ ,  $\text{Fe}_2\text{O}_3$ ,  $\text{NiO}$ ,  $\text{CuO}$  and  $\text{Na}_2\text{CO}_3$  were used as starting materials. These powders were weighted to a prescribed ratio, mixed and ground in an agate mortar with methanol. The mixtures were dried and calcined at 1273 K for 20 h in air. The obtained powders were ground and pressed into pellets and sintered at 1273 K for 40 h in  $\text{O}_2$  flow. These pellets were cut into rectangular-shaped specimens of  $1 \times 1 \times 10 \text{ mm}^3$  for measurements of  $\rho$  and  $S$ .

Crystallographic structure analysis was performed by X-ray diffraction (XRD) using  $\text{CuK}\alpha$  radiation. Diffraction patterns were treated with the analysis program *JANA2000* for lattice parameter refinement [12]. Sample microstructures were observed by scanning electron microscopy (SEM).  $\rho$  Was measured in air in the temperature range of 300–1073 K using a conventional four-probe dc technique.  $S$  was calculated from a plot of thermoelectric voltage against temperature differential as measured in air at 373–1073 K using an instrument designed by our laboratory. Two Pt–Pt/Rh (R-type) thermocouples were attached to both ends of the sample using Ag paste and the Pt wires of the thermocouples used as voltage terminals. Measured  $S$  values were subtracted from those of the Pt wires to obtain the net  $S$  values of the samples.

## 3. Results and discussion

XRD measurements were performed on the polished surface of each sintered pellet. As shown in Fig. 1, the XRD patterns of all the samples can be seen to agree with the reported data for Co326 structure [13], with the exception of the weak diffraction peaks from secondary phases of  $\text{CoNiO}_2$  and  $\text{CaO}$  in the Ni-substituted sample [14]. Since these secondary phases could not be eliminated by optimizing sintering conditions and reducing the amount of Ni, the Co site seems to be difficult to substitute with Ni. Refined cell parameters are listed in Table 1. Both  $a$  and  $c$  parameters are increased by the Mn substitution and the only  $c$  parameter is increased by the Cu substitution. However, the lattice parameter changes for the other substitutions are small because the ionic radius of

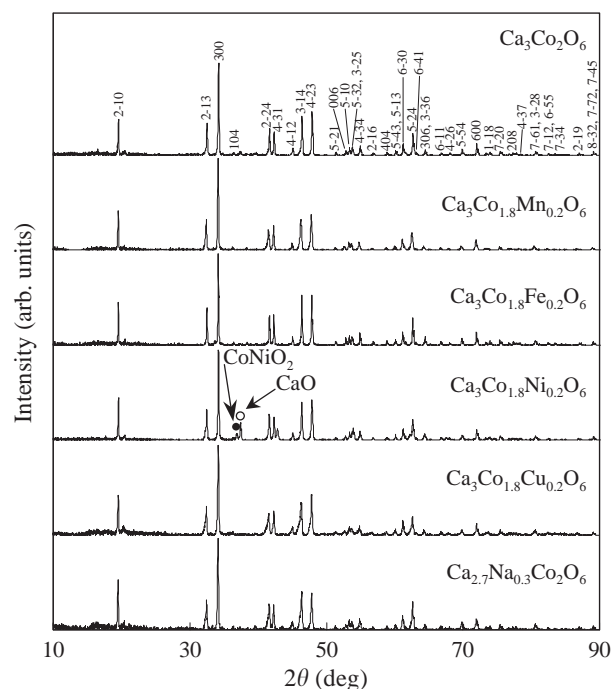


Fig. 1. XRD patterns ( $\text{CuK}\alpha$  radiation) diffracted from the surfaces of  $\text{Ca}_3\text{Co}_{1.8}\text{M}_{0.2}\text{O}_6$  ( $M = \text{Mn, Fe, Co, Ni and Cu}$ ) and  $\text{Ca}_{2.7}\text{Na}_{0.3}\text{Co}_2\text{O}_6$  pellets.

substitution elements are almost the same size as the original ones.

Fig. 2 shows SEM images of fracture cross-sections of the samples. It can be seen that the non-substituted Co326 is constructed of grains several  $\mu\text{m}$  in size. When compared with this microstructure, the grain size of the Mn- and Fe-substituted samples is small. Therefore, an effect of the Mn and Fe substitutions is a reduction of grain growth by solid-state reaction. Conversely, the grain size of Cu- and Na-substituted samples is several times larger than non-substituted Co326. In addition, since the grains are well connected in the Cu-substituted sample, the effects of the substitution seem to be reduction of the melting temperature and enhancement of the solid-state reaction. On the other hand, grains of the Na-substituted Co326 tend to form a polyhedral shape, while grains of the non-substituted Co326 tend to have a spherical shape. This change of the grain shape indicates that the growth rate of the grains is enhanced by the presence of  $\text{NaO}$  or  $\text{Na}_2\text{CO}_3$ , which can play the role of a solvent for the cobaltite and induce a partial liquid-phase reaction. Moreover, as seen in the white circle of Fig. 2(f), a small number of platelet-shaped particles are combined with spherical-shaped grains. Since the amount of platelets was increased with increasing Na content (data not shown), a secondary phase of  $\text{Na}_x\text{CoO}_2$ , which tends to form platelet-shaped particles derived from the layered crystallographic structure, seems to be present in the  $\text{Ca}_{2.7}\text{Na}_{0.3}\text{Co}_2\text{O}_6$

Table 1

Refined lattice parameters of  $\text{Ca}_3\text{Co}_{1.8}\text{M}_{0.2}\text{O}_6$  ( $M = \text{Mn, Fe, Co, Ni}$  and  $\text{Cu}$ ) and  $\text{Ca}_{2.7}\text{Na}_{0.3}\text{Co}_2\text{O}_6$  pellets

Composition	$c$ (nm)	$a$ (nm)
$\text{Ca}_3\text{Co}_{1.8}\text{Mn}_{0.2}\text{O}_6$	9.0889(1)	10.4311(2)
$\text{Ca}_3\text{Co}_{1.8}\text{Fe}_{0.2}\text{O}_6$	9.0812(1)	10.3828(1)
$\text{Ca}_3\text{Co}_2\text{O}_6$	9.0769(1)	10.3816(1)
$\text{Ca}_3\text{Co}_{1.8}\text{Ni}_{0.2}\text{O}_6$	9.0761(4)	10.3777(6)
$\text{Ca}_3\text{Co}_{1.8}\text{Cu}_{0.2}\text{O}_6$	9.0772(4)	10.4074(2)
$\text{Ca}_{2.7}\text{Na}_{0.3}\text{Co}_2\text{O}_6$	9.0737(5)	10.3839(6)

(Space group:  $R\bar{3}c$ ,  $Z = 6$ ).

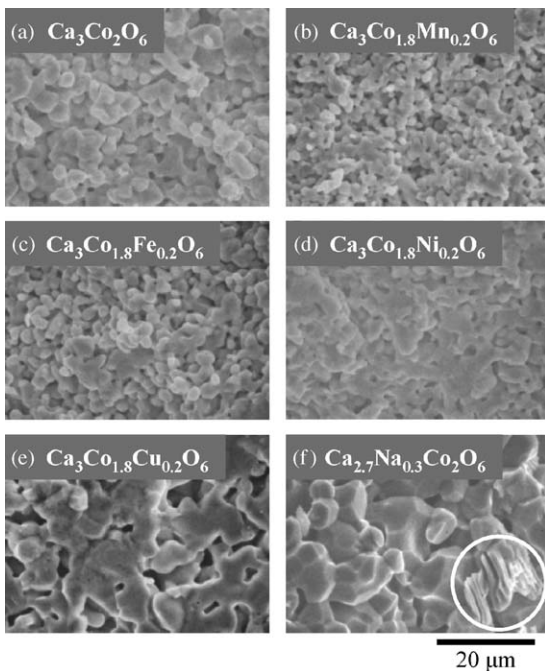


Fig. 2. SEM images of fracture cross-sections of  $\text{Ca}_3\text{Co}_{1.8}\text{M}_{0.2}\text{O}_6$  ( $M = \text{Mn, Fe, Co, Ni}$  and  $\text{Cu}$ ) and  $\text{Ca}_{2.7}\text{Na}_{0.3}\text{Co}_2\text{O}_6$  pellets.

compound, although the diffraction peaks of the  $\text{Na}_x\text{CoO}_2$  phase could not be observed in the XRD pattern.

From these results of crystallographic structure analysis and microstructural observation, with the exception for the Ni and Na substitution, it was confirmed that the single-phase  $\text{Ca}_3\text{Co}_{2-x}\text{M}_x\text{O}_6$  had been obtained. Moreover, the number of platelet-shaped  $\text{Na}_x\text{CoO}_2$  particles is small and the  $a$  cell parameter shrinks by the Na substitution, it would appear that the larger component of Na substitutes the Ca site of the Co326 phase.

The  $T$  dependence of  $\rho$  is shown in Fig. 3. A thermally activated behavior is observed in each sample over the entire measured temperature range. However, the plots of the relationship between  $\log \rho$  and  $1000/T$  is not on the straight line, particularly in the high temperature region above 500 K. Though the origin of this change in

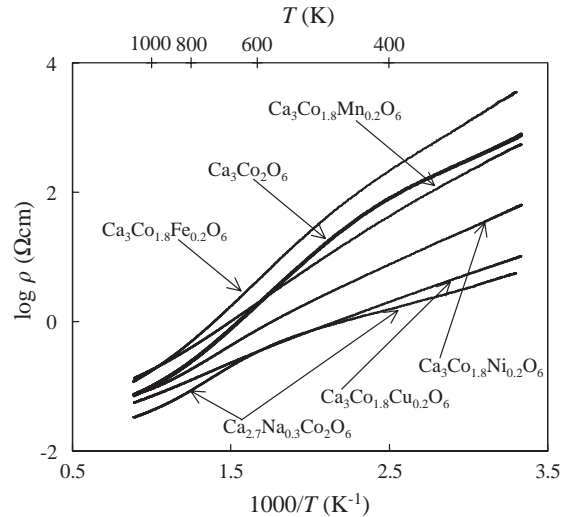


Fig. 3. Relationship of  $\log \rho$  and  $1000/T$  in  $\text{Ca}_3\text{Co}_{1.8}\text{M}_{0.2}\text{O}_6$  ( $M = \text{Mn, Fe, Co, Ni}$  and  $\text{Cu}$ ) and  $\text{Ca}_{2.7}\text{Na}_{0.3}\text{Co}_2\text{O}_6$  pellets.

the plot slope has yet to be elucidated, we suppose that this behavior is not due to the phase transition nor the oxygen loss, because the thermogravimetry and the differential thermal analysis indicate no significant indication of the changes in the  $\rho$ -measurement temperature range, but rather is due to the complicated band structure derived from the highly anisotropic crystallographic structure of the Co326 phase. In addition, the grain boundary effect and the impurity phase, especially in the Ni- and Na-substituted samples, would make the nature of  $T$  dependence complex. The value of  $\rho$  in every sample decreases rapidly with increasing temperature. For instance,  $\rho$  in the non-substituted sample decreases from  $8 \times 10^5$  to  $80 \text{ m}\Omega \text{ cm}$  over the temperature range of 300–1073 K. Since a thermoelectric material requires low  $\rho$ , the Co326 system can be expected to provide good thermoelectric performance at high temperatures.

As shown in Fig. 4, the  $T$  dependence of  $S$  in every sample indicates a thermally activated behavior, which is consistent with the measured  $\rho$  values. However, the activation energy calculated from the relationship  $S$  vs.  $1/T$  ( $E_S$ ) is much smaller than that derived from  $T$ -dependence of  $\rho$  ( $E_\rho$ ) in every sample as listed in Table 2. This would suggest a polaron conduction and the difference in magnitude corresponds to the hopping energy, which contributes to the change of mobility by  $T$ . While the Fe substitution can increase the value of  $S$ , the Cu, Mn and Na substitutions decrease it at temperatures below 673 K. Moreover, the Ni substitution has little effect on the  $S$  value. Although  $S$  decreases with increasing temperature, all samples exhibit a large  $S$  value of more than  $160 \mu\text{V/K}$ , even at temperatures as high as 1073 K. Since  $\rho$  rapidly decreases with increasing temperature as mentioned above, the Co326 system has potential as a high-temperature thermoelectric material.

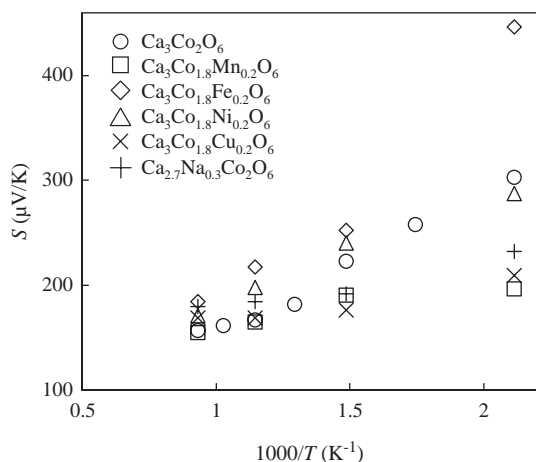


Fig. 4. Relationship of  $S$  and  $1000/T$  in  $\text{Ca}_3\text{Co}_{1.8}\text{M}_{0.2}\text{O}_6$  ( $M = \text{Mn}$ ,  $\text{Fe}$ ,  $\text{Co}$ ,  $\text{Ni}$  and  $\text{Cu}$ ) and  $\text{Ca}_{2.7}\text{Na}_{0.3}\text{Co}_2\text{O}_6$  pellets.

Table 2

Activation energies calculated from the gradients of linear fitted lines for  $\log \rho$  vs.  $1000/T$  plots ( $E_\rho$ ) in the temperature region of 450–950 K and for  $S$  vs.  $1000/T$  ( $E_S$ ) at 673–1073 K

Composition	$E_\rho$ (eV)	$E_S$ (eV)
$\text{Ca}_3\text{Co}_{1.8}\text{Mn}_{0.2}\text{O}_6$	0.32	0.066
$\text{Ca}_3\text{Co}_{1.8}\text{Fe}_{0.2}\text{O}_6$	0.44	0.12
$\text{Ca}_3\text{Co}_2\text{O}_6$	0.42	0.13
$\text{Ca}_3\text{Co}_{1.8}\text{Ni}_{0.2}\text{O}_6$	0.27	0.13
$\text{Ca}_3\text{Co}_{1.8}\text{Cu}_{0.2}\text{O}_6$	0.20	0.036
$\text{Ca}_{2.7}\text{Na}_{0.3}\text{Co}_2\text{O}_6$	0.25	0.022

Let us focus on the effect of substitution on  $\rho$  and  $S$  values. In the lower temperature region below 673 K, with the exception of Fe, substitution of elements is effective in reducing  $\rho$ . Since  $S$  is decreased by the Mn, Cu and Na substitutions, the reduction of  $\rho$  in these three samples is caused by the injection of carriers. Conversely, a simultaneous increase in  $\rho$  and  $S$  in the Fe-substituted sample indicates a reduction in carrier density. Moreover, since the Na-substituted sample has a smaller  $\rho$  value than the non-substituted one whereas  $S$  is almost the same above 873 K, the carrier mobility is improved by this substitution. While acknowledging that the secondary phase of the layered-cobaltite  $\text{Na}_x\text{CoO}_2$ , which has a much lower  $\rho$  than the  $\text{Co}_3\text{O}_2$  phase, could also contribute to the reduction of  $\rho$  in the Na-substituted sample, we propose that this enhancement of the carrier mobility is not only caused by the intrinsic substitution effect but is also related to the modification of the microstructure, i.e., the enhancement of grain size and grain boundary connectivity (as shown in Fig. 2), which can reduce the energy barriers associated with grain boundaries. Additionally, the significant reduction of  $\rho$  as a result of Cu substitution

could be also related to the modification of the microstructure. It might appear that the grain size generally has little influence on the  $\rho$  value if the mean free path of the carrier is much smaller than the grain size. However,  $\rho$  along the  $ab$ -plane is one or two orders of higher than that along  $c$ -axis because of the highly anisotropic crystallographic structure of  $\text{Co}_3\text{O}_2$ . In this case, the energy loss of the transport carriers at the grain boundary consisting of grains having the different crystallographic orientation could be much higher than that at the boundary between grains, which face in the same crystallographic axis. Therefore, the number of the grain boundaries and the connectivity of the grains could have a larger impact on the  $\rho$  value of the polycrystalline  $\text{Co}_3\text{O}_2$  than the materials having the isotropic crystallographic structure.

The thermoelectric power factor ( $\text{PF} = S^2/\rho$ ) was calculated from measured  $\rho$  and  $S$  values (Fig. 5). The PF value in every sample increases with increasing temperature. This  $T$  dependence is mainly caused by the significant reduction of  $\rho$  at high temperatures. Although  $S$  is improved by the Fe substitution, the increase in  $\rho$  prevents the improvement of PF. With the exception of the Cu-substituted sample at temperatures below 673 K, the Cu and Na substitutions can enhance PF because of the reduction of  $\rho$  without the serious degradation of  $S$ . This is especially so in the case of the Na-substituted sample above 873 K, where the PF value is more than two times larger than the non-substituted one due to the significant reduction of  $\rho$ . We propose that the enhancement of PF is related to the above-mentioned microstructure modification, although investigations of single-crystal specimens will be required to elucidate the substitution effects in greater detail.

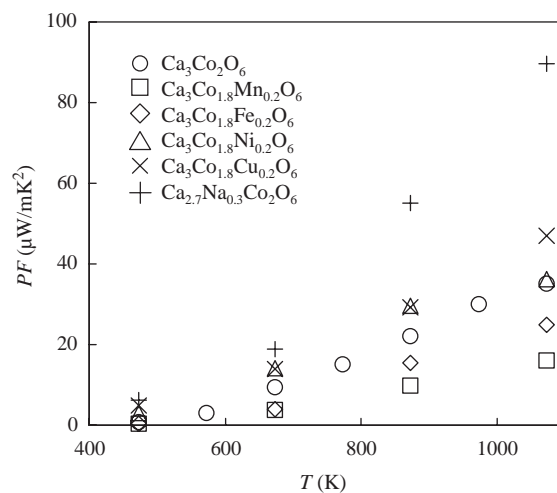


Fig. 5. Temperature dependence of PF in  $\text{Ca}_3\text{Co}_{1.8}\text{M}_{0.2}\text{O}_6$  ( $M = \text{Mn}$ ,  $\text{Fe}$ ,  $\text{Co}$ ,  $\text{Ni}$  and  $\text{Cu}$ ) and  $\text{Ca}_{2.7}\text{Na}_{0.3}\text{Co}_2\text{O}_6$  pellets.

#### 4. Conclusions

The effect of partial element substitution on the thermoelectric properties of Co326 was investigated. Transition-metal substitutions at the Co site affect carrier density, resulting in an increase in  $S$  and  $\rho$  in the case of Fe substitution, and a decrease in  $S$  and  $\rho$  in the case of Mn, Cu and Na substitutions. Since  $\rho$  is significantly reduced by the partial substitution of Na at the Ca site without the degradation of  $S$ , PF is improved and reaches  $90 \mu\text{W}/\text{mK}^2$  at 1073 K. We propose that not only the intrinsic substitution effect on the electronic state but also the effects of substitutions on the microstructure, such as the increase in the grain size and the reduction in the number of grain boundaries due to the Cu and Na substitutions, can contribute to the PF enhancement of bulk Co326 materials. The  $ZT$  of Na-substituted Co326 is calculated to be 0.04 at 1073 K using the  $\kappa$  value of the single-crystal Co326 along the  $c$ -axis,  $2.4 \text{ W}/\text{mK}$  [7]. Although this  $ZT$  value is not enough for the practical application, the Na-substituted Co326 could have the higher  $ZT$  value because the polycrystalline material generally has lower  $\kappa$  than single crystal. Moreover, since the PF increases with the temperature and the reported  $T$  dependence of  $\kappa$  value linearly decreases with the increase of the temperature [7], Co326 is expected to possess high thermoelectric efficiency at higher temperatures. Since it was confirmed that the Co326 is chemically stable up to 1300 K [6] and the conventional thermoelectric semiconductors usually deteriorate by the oxidation at high temperature in air, the title compound could be considered a potential

candidate for use as a thermoelectric material at high temperatures in air.

#### References

- [1] I. Terasaki, Y. Sasago, K. Uchinokura, Phys. Rev. B 56 (1997) 12685–12687.
- [2] K. Fujita, T. Mochida, K. Nakamura, Jpn. J. Appl. Phys. 40 (2001) 4644–4647.
- [3] S. Li, R. Funahashi, I. Matsubara, K. Ueno, H. Yamada, J. Mater. Chem. 9 (1999) 1659–1660.
- [4] R. Funahashi, I. Matsubara, H. Ikuta, T. Takeuchi, U. Mizutani, S. Sodeoka, Jpn. J. Appl. Phys. 39 (2000) L1127–L1129.
- [5] M. Shikano, R. Funahashi, Appl. Phys. Lett. 82 (2003) 1851–1853.
- [6] E. Woermann, A. Muan, J. Inorg. Nucl. Chem. 32 (1970) 1455–1459.
- [7] M. Mikami, R. Funahashi, M. Yoshimura, Y. Mori, T. Sasaki, J. Appl. Phys. 94 (2003) 6579–6582.
- [8] K. Iwasaki, H. Yamane, S. Kubota, J. Takahashi, M. Shimada, J. Alloys Compd. 358 (2003) 210–215.
- [9] A. Maignan, S. Hébert, C. Martin, D. Flahaut, Mater. Sci. Eng. B 104 (2003) 121–125.
- [10] J. An, C.W. Nan, Solid State Commun. 129 (2004) 51–56.
- [11] M. Mikami, R. Funahashi, Trans. Mater. Res. Soc. Jpn. 29 (2004) 2773–2776.
- [12] V. Petricek, M. Dusek, L. Palatinus, Jana 2000, Institute of Physics, Praha, Czech Republic, 2000.
- [13] H. Fjellvåg, E. Gulbrandsen, S. Aasland, A. Olsen, B.C. Hauback, J. Solid State Chem. 124 (1996) 190–194.
- [14] In Ref. [11], we reported the presence of a  $\text{Cu}_2\text{O}$  impurity phase in  $\text{Ca}_3\text{Co}_{1.8}\text{Cu}_{0.2}\text{O}_6$  sintered in air, however, this impurity phase can be eliminated by sintering in an  $\text{O}_2$  flow. In addition,  $\text{Ca}_3\text{Co}_{1.8}\text{Ni}_{0.2}\text{O}_6$  in the previous report contained the  $\text{Ca}_3\text{Co}_4\text{O}_9$  phase, resulting in much lower  $\rho$  values than the present study.